Journal of ELECTRONIC MATERIALS, Vol. 47, No. 2, 2018
DOI: 10.1007/s11664-017-5896-8

X-ray Diffraction and Magnetic Investigations of Lithium-Zinc Ferrites Synthesized by Electron Beam Heating

A.P. SURZHIKOV,[1] E.N. LYSENKO,[1] E.A. SHEVELEVA,[1] A.V. MALYSHEV,[1] A.L. ASTAFYEV,[1] and V.A. VLASOV[1,2]

1.—Problem Research Laboratory of Electronics, Dielectrics and Semiconductors, Tomsk Polytechnic University, Tomsk, Russia 634050. 2.—e-mail: vlvitan75@mail.ru

$Li_{0.5(1-x)}Zn_xFe_{2.5-0.5x}O_4$ ferrites (x = 0.2; 0.4) were produced by thermal and radiation-thermal (RT) synthesis from Li_2CO_3-Fe_2O_3-ZnO powder mixtures and then studied using x-ray diffraction (XRD) and saturation magnetization analysis. The RT synthesis was carried out by 2.4 MeV electron beam heating of samples from the first batch at the temperatures of 600°C, 700°C, 750°C and isothermal exposure time of 0 min, 10 min, 20 min, 30 min, 60 min, and 120 min. For comparative analysis, thermal heating of samples from the second batch was performed in a resistance laboratory furnace using the same time and temperature regimes. XRD analysis of samples showed the formation of lithium-zinc ferrites with greater homogeneous phase composition at lower values of temperature and time during RT synthesis compared to the samples obtained by thermal heating. Also, RT-synthesized ferrites are characterized by significantly higher values of saturation magnetization at all time and temperature regimes. It was established that a regime of RT synthesis at 750°C–30 min provides the formation of lithium-zinc ferrites with a high degree of final phase composition.

Key words: Lithium-zinc ferrites, radiation-thermal synthesis, electron beam heating, x-ray diffraction analysis, magnetic properties, saturation magnetization

INTRODUCTION

Ferrites are widely used as magnetic materials in radio-electronics, engineering and computer applications, due to a combination of high magnetization and semiconductor or dielectric (insulator) properties.[1–4] In particular, the substituted lithium ferrites, in which Fe^{3+} ions are partially replaced by Zn^{2+} ions, are utilized in microwave applications due to their low costs and excellent ferromagnetic properties with high values of Curie temperature and saturation magnetization.[5–12] The essential condition for determining the high levels of the desirable properties of lithium ferrite materials is the homogeneity of chemical and phase composition in the synthesized products.

(Received April 19, 2017; accepted October 23, 2017; published online November 6, 2017)

Some special methods are known to improve the efficiency of solid-phase synthesis. Among these, microwave and mechanochemical treatments permit the activation of the reactants during synthesis.[13–17] Although there are some disadvantages, such as contamination of ferrite powders by materials of grinding balls in the case of mechanochemical treatment[17] or microwave treatment, there is dependence on ferrite dielectric properties.[18,19]

In, Refs. 20–23 it was demonstrated that radiation-thermal (RT) heating of ferrite materials by high-power beams of above 1 MeV accelerated electrons is an effective method for intensifying solid-state reactions and increasing phase composition homogeneity. The RT method has been successfully applied for the preparation of some ferrite materials, such as NiZn ferrites,[24] strontium ferrites,[25] hexaferrites[26,27] and substituted Li ferrites, which were obtained by either RT powder synthesis[28–30] or

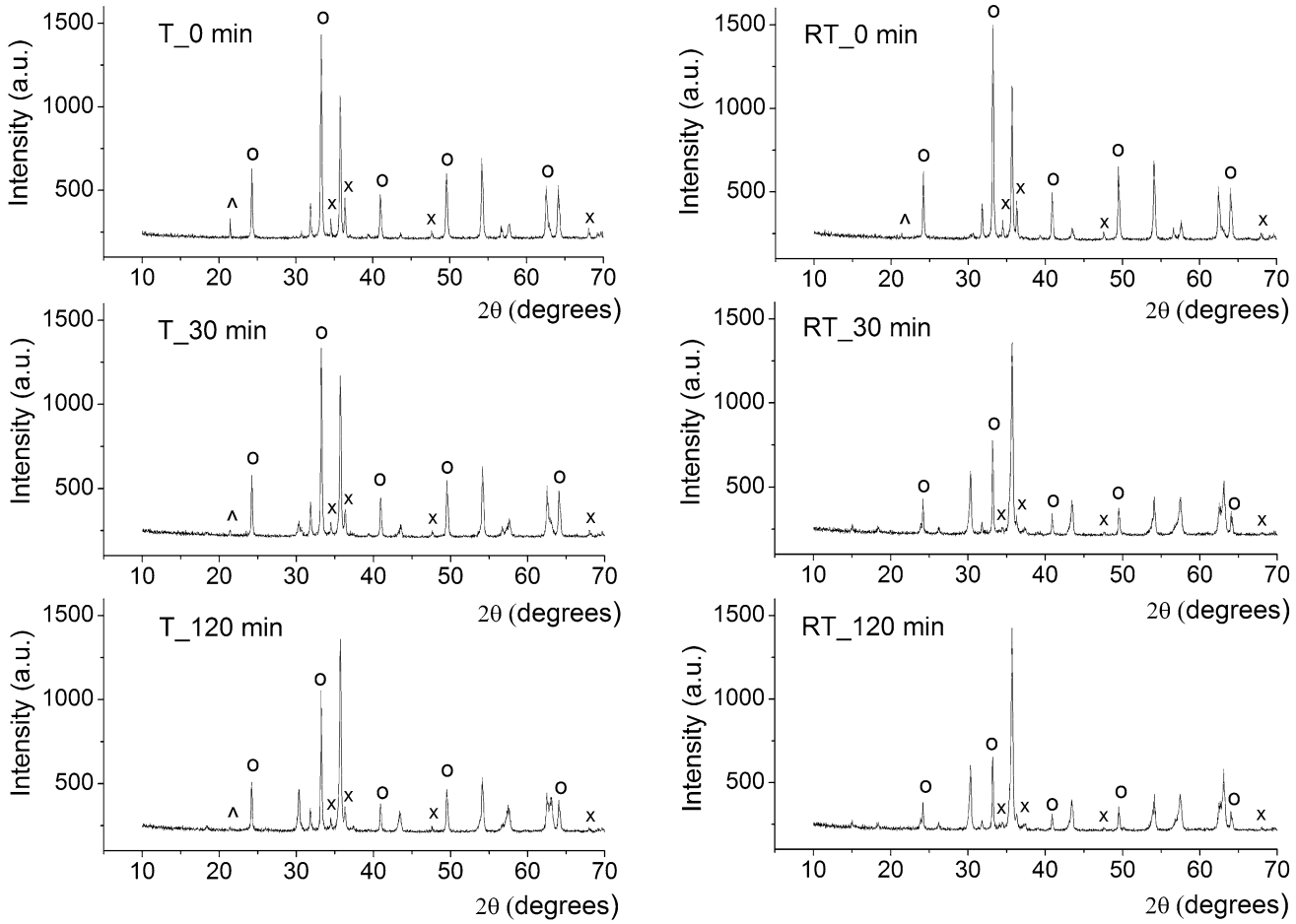

Fig. 1. XRD patterns for $Li_{0.5(1-x)}Zn_xFe_{2.5-0.5x}O_4$ (x = 0.2) synthesized under conditions of T and RT annealing at 600°C and 0 min, 30 min, and 120 min. The markers of Fe_2O_3 (O), Li_2CO_3 (^) and ZnO (x) are indicated.

RT ceramics sintering.[31] According to x-ray diffraction (XRD) and thermogravimetric analysis of RT-synthesized LiZn[28] and LiTi ferrites,[29,30] the observed radiation-thermal effect results in intensification of the solid-phase process, which significantly decreases the temperature and time rewquired for ferrite synthesis compared to conventional thermal heating in high-temperature furnaces. Moreover, as was shown in, Ref. 29 ferrites can be obtained by using two types of high-energy electron heating (pulsed or continuous) that extend the possibility of using radiation-thermal technology for lithium-substituted ferrite production.

In, Ref. 30 the saturation magnetization results confirmed high efficiency of LiTi ferrite synthesis using RT heating of the reaction mixture. However, the magnetic properties of LiZn ferrites obtained by RT heating were not extensively investigated.

In this paper, we report a magnetization study of the solid-state formation of lithium-zinc ferrites synthesized by a 2.4 MeV pulse electron beam. The results are compared with the magnetization of LiZn ferrites synthesized by conventional solid-state synthesis in the laboratory furnace using similar time–temperature regimes.

EXPERIMENTAL PROCEDURE

Lithium-zinc ferrites with $Li_{0.5(1-x)}Zn_x$-$Fe_{2.5-0.5x}O_4$ (where x = 0.2; 0.4) chemical compositions were synthesized from a Li_2CO_3-ZnO-Fe_2O_3 mechanical mixture of reagents, which were produced by weighing the required amounts of predried components and then mixing them in an agate mortar. For the synthesis, the samples were compacted in tablet form with 15 mm diameter and 2 mm thickness by 200 MPa single-ended cold pressing. The samples were divided into two batches for the RT and T syntheses.

RT synthesis of samples from the first batch was carried out using a pulse electron accelerator ILU-6 with 2.4 MeV electron energy and 400 mA pulse

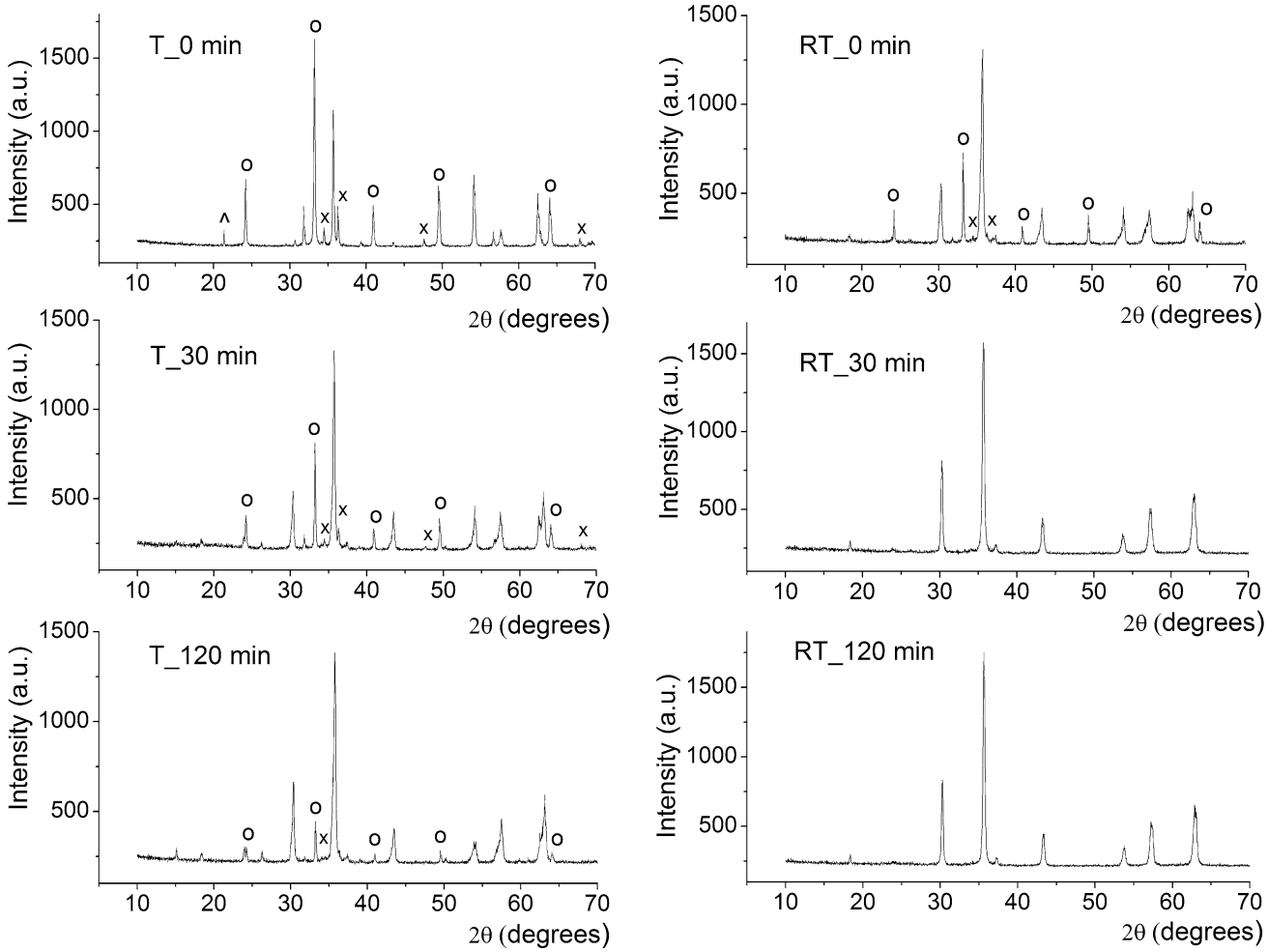

Fig. 2. XRD patterns for $Li_{0.5(1-x)}Zn_xFe_{2.5-0.5x}O_4$ (x = 0.2) synthesized under conditions of T and RT annealing at 700°C and 0 min, 30 min, and 120 min. The markers of Fe_2O_3 (O), Li_2CO_3 (^) and ZnO (x) are indicated.

beam current.[32–34] RT processing regimes are regulated by the pulse repetition frequency of the electron beam, allowing any changes in the temperature regime and heating rates. The samples were heated up to the synthesis temperatures of 600°C, 700°C and 750°C by the electron beam in air using a special cell made from lightweight fireclay with thermally insulating walls and lid that were transparent to the electron beam. The temperature was controlled by a type S thermocouple located in a control sample which was placed near the investigated samples. The times of isothermal synthesis were 0 min, 10 min, 20 min, 30 min, 60 min, and 120 min, and the duration of non-isothermal heating and cooling stages did not exceed 3 min.

The thermal synthesis of samples from the second batch was performed in a high-temperature laboratory furnace at similar time–temperature regimes.

The phase composition of the synthesized samples was controlled using ARL X'TRA x-ray diffractometer with a Peltier Si(Li) semiconductor detector and Cuk_α radiation. XRD patterns were measured for $2\theta = (10 \div 70)°$ with a scan rate of 0.02°/s. The phase compositions of the samples were identified using the PDF-4 + powder database of the International Center for Diffraction Data (ICDD). Lattice parameters specified the zinc content in the synthesized LiZn ferrites for lithium-zinc ferrites.[28] XRD patterns were processed by full-profile analysis using Powder Cell 2.5 software.

For the saturation magnetization study, parallelepipeds with the size of 2x2x8 mm^3 were made from the synthesized samples and measured by a vibrating sample magnetometer with the maximum field of 10 kOe.

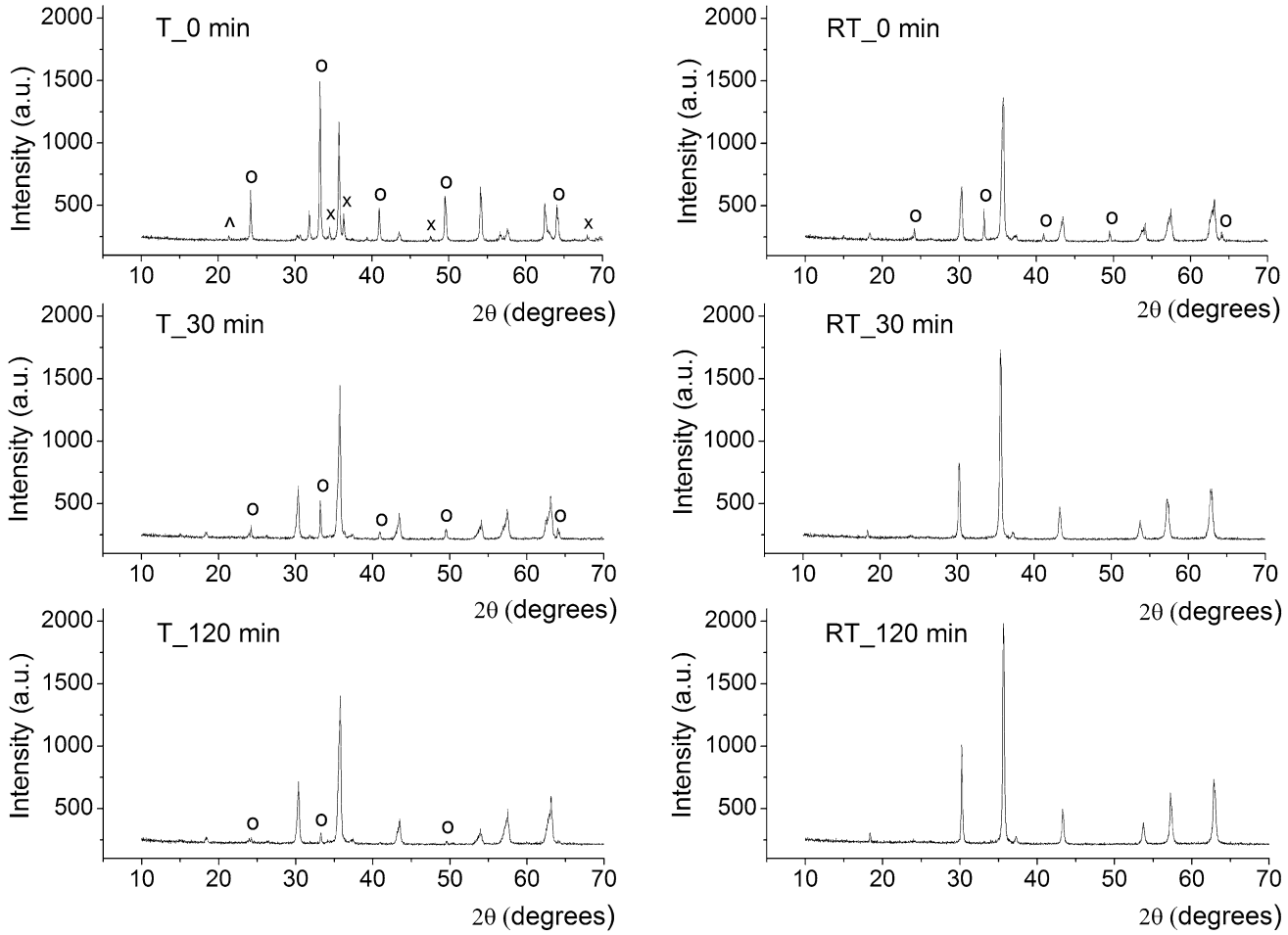

Fig. 3. XRD patterns for $Li_{0.5(1-x)}Zn_xFe_{2.5-0.5x}O_4$ (x = 0.2) synthesized under conditions of T and RT annealing at 750°C and 0 min, 30 min, and 120 min. The markers of Fe_2O_3 (O), Li_2CO_3 (^) and ZnO (x) are indicated.

RESULTS AND DISCUSSION

X-ray Diffraction Analysis

XRD results were obtained for all samples synthesized at different temperature–time regimes. However, the present article cites selective XRD patterns, which are the most important from our point of view. Figures 1 and 2 show the XRD patterns for $Li_{0.5(1-x)}Zn_xFe_{2.5-0.5x}O_4$ (x = 0.2) samples synthesized by T and RT heating at 600°C (Fig. 1), 750°C (Fig. 2) at synthesis times of 0 min, 30 min, and 120 min.

The XRD patterns for T and RT-synthesized samples at 600°C (Fig. 1) indicate the reflections from ZnO, α-Fe_2O_3, and Li_2CO_3 initial reagent phases (marked reflection in Fig. 1) that have not completely reacted with each other, and a superposition of spinel phase reflections associated with pure lithium ferrites and/or substituted by zinc lithium ferrites (unmarked reflections in Fig. 1, occur primarily at 2θ = 30.3°, 43°). Unmarked reflections at 2θ = 35.5° and 54° correspond to both α-Fe_2O_3 and spinel phases, from which the reflections merge into single-peak reflections. According to the study of phase formation in Li_2CO_3-ZnO-Fe_2O_3 systems during lithium-zinc ferrites synthesis using thermogravimetric and calorimetric analysis, the observed spinel phases are associated with the transient phase formation of the pure lithium ferrite, $Li_{0.5}Fe_{2.5}O_4$, and lithium-zinc ferrites with close values of lattice parameters, $Li_{0.5(1-x)}Zn_xFe_{2.5-0.5x}O_4$ ($0 < x < 0.6$). The peak intensity of spinel phases increases with increasing synthesis time, while the peak intensity of initial reagents decreases.

With the increase in the synthesis temperature up to 700°C and 750°C, the initial reagents are still observed in the samples synthesized at thermal

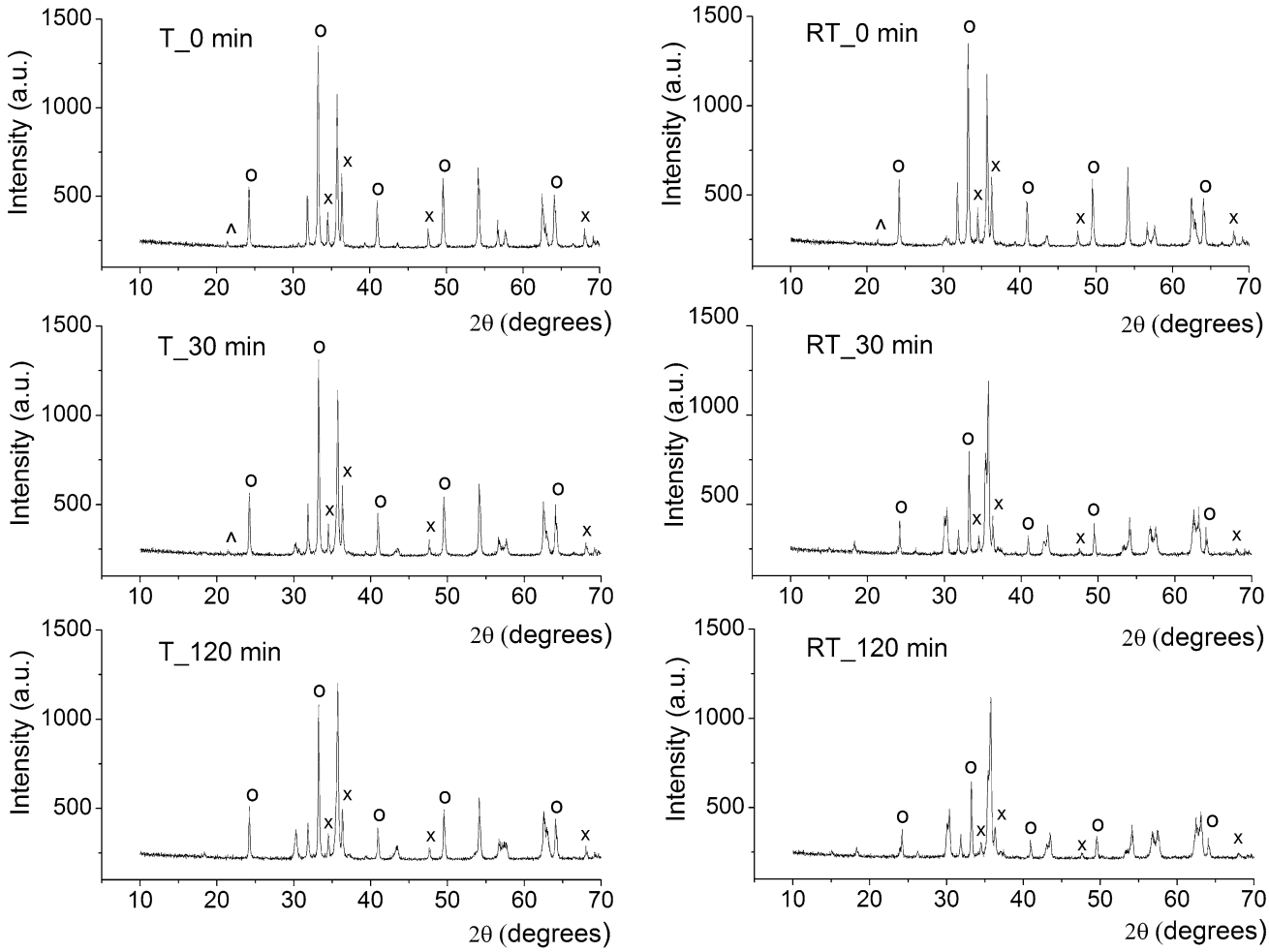

Fig. 4. XRD patterns for $Li_{0.5(1-x)}Zn_xFe_{2.5-0.5x}O_4$ (x = 0.4) synthesized under conditions of T and RT annealing at 600°C and 0 min, 30 min, and 120 min. The markers of Fe_2O_3 (O), Li_2CO_3 (^) and ZnO (x) are indicated.

heating at all synthesis time periods, and in the samples synthesized by the RT mode that includes only the non-isothermal stage of heating. However, the samples which were synthesized via RT annealing for 30 min and more are characterized by the presence of spinel phases only.

Figures 3 and 4 show the XRD patterns for $Li_{0.5(1-x)}Zn_xFe_{2.5-0.5x}O_4$ (x = 0.4) ferrite synthesized in T and RT modes at 600°C (Fig. 3) and 750°C (Fig. 4) at synthesis times of 0 min, 30 min, and 120 min. Following XRD results, the regularities of phase formation in Li_2CO_3-ZnO-Fe_2O_3 systems with x = 0.4 at both T and RT regimes are similar to the above results for the synthesis of lithium-zinc ferrite with x = 0.2. At low 600°C synthesis temperature, the samples are characterized by inhomogeneous phase composition, including non-reacted precursors. The phases with high concentration of spinel ferrite are formed in the samples synthesized by RT heating at 750°C for 30 min and more.

Saturation Magnetization Analysis

Saturation magnetization for $Li_{0.5(1-x)}Zn_xFe_{2.5-0.5x}O_4$ with x = 0.2 and 0.4 as a function of synthesis time is presented in Fig. 5. The curves are characterized by a rapid increase in magnetization for the samples synthesized during the first 30 min and a slight growth in magnetization at further heating stages. As was shown in Ref. 28 by thermomagnetometric and calorimetric analysis, the first stage is related to the rapid formation of pure lithium spinel ferrite. By increasing synthesis reaction time, interactions between lithium ferrite and residual amounts of reagent oxides occur, leading to LiZn spinel ferrite formation. Consequently, a slight increase in the magnetization of the samples is observed due to higher magnetization values of LiZn ferrites compared to $Li_{0.5}Fe_{2.5}O_4$ (Figs. 6, 7).

According to Neel's theory,[35] a tetrahedral diamagnetic substitution of iron cations by zinc ions of

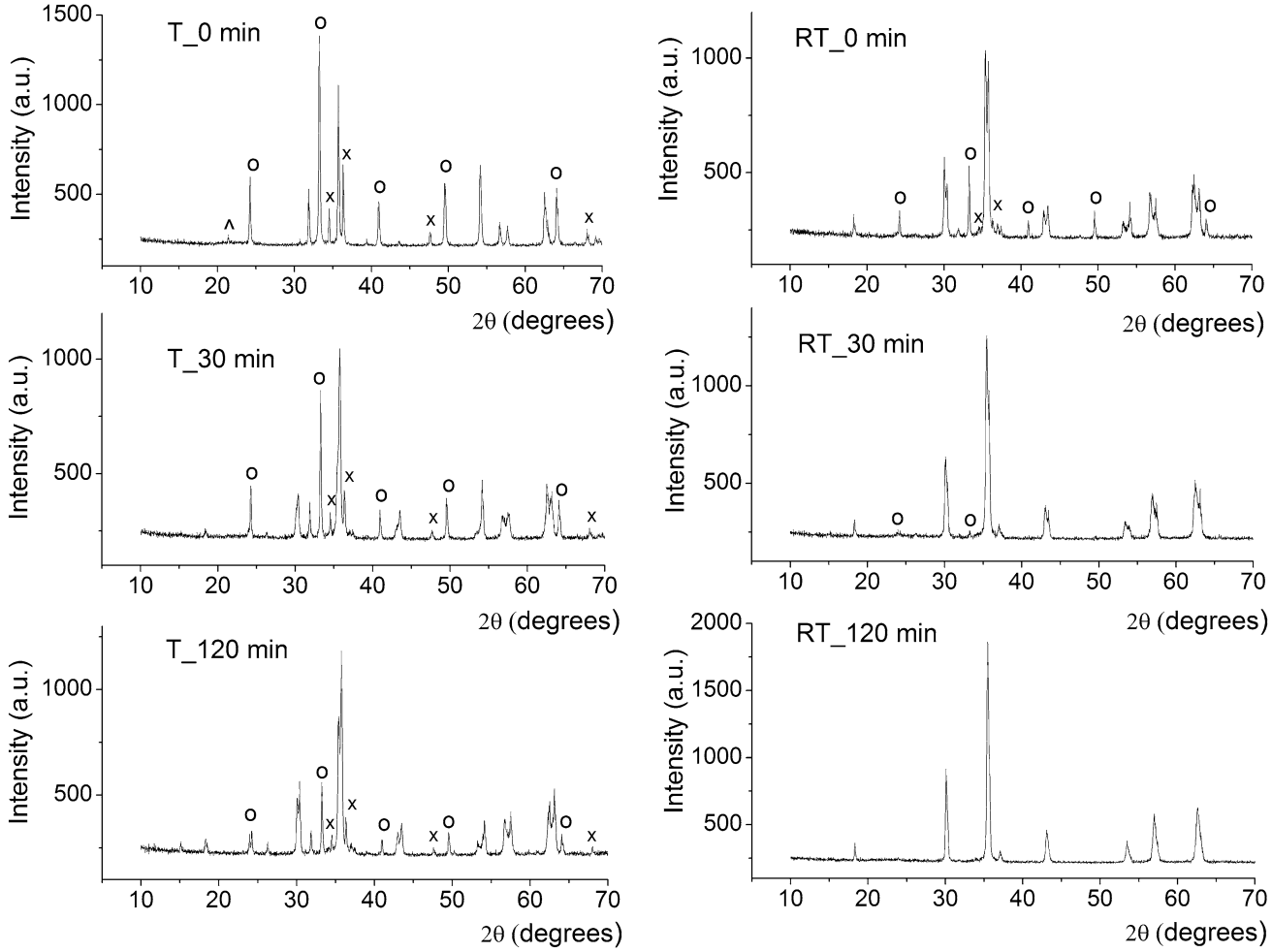

Fig. 5. XRD patterns for $Li_{0.5(1-x)}Zn_xFe_{2.5-0.5x}O_4$ (x = 0.4) synthesized under conditions of T and RT annealing at 700°C and 0 min, 30 min, and 120 min. The markers of Fe_2O_3 (O), Li_2CO_3 (^) and ZnO (x) are indicated.

small concentrations increases the magnetization of domains, but at $x > 0.3$ in $Li_{0.5(1-x)}Zn_xFe_{2.5-0.5x}O_4$. The replacement leads to a high reduction in exchange interaction between sublattices and partial disorientation of magnetic moments in domains and, consequently, decreased saturation of ferrite magnetization. This explains the lower values of saturation magnetization in the ferrite with x = 0.4 compared to x = 0.2. This is confirmed by the results from, Refs. 36–39 where the magnetization of LiZn ferrites was studied.

Regardless of zinc content in the samples, RT-synthesized samples are characterized by significantly higher values of saturation magnetization in comparison with samples obtained by thermal heating. By increasing the synthesis temperature up to 750°C, the samples reach high values of magnetization at the isothermal stage onset. At longer isothermal exposure of 30 min and more, the RT synthesis process produces LiZn ferrites with magnetization values that are close to nominal characteristics used in ferrite production.

The radiation-thermal effect in ferrite synthesis can be explained in terms of the surface-recombination mechanism of high-temperature radiation-induced mass transfer in ion structures proposed in Ref. 40. The regions of structural failure in heterogeneous structures are characterized by a higher rate of non-radiative electron–hole and exciton recombination compared to that in the volume that causes local temperature gradients, defects and stresses. This process intensifies mass transfer at interphase boundaries, and, as a result, it can accelerate the formation of ferrites.

In addition, because of the high concentration of free electrons in the ferrite caused by a beam of accelerated electrons, a short-term decrease in the charge of multiply charged cations (Fe^{3+}) can occur

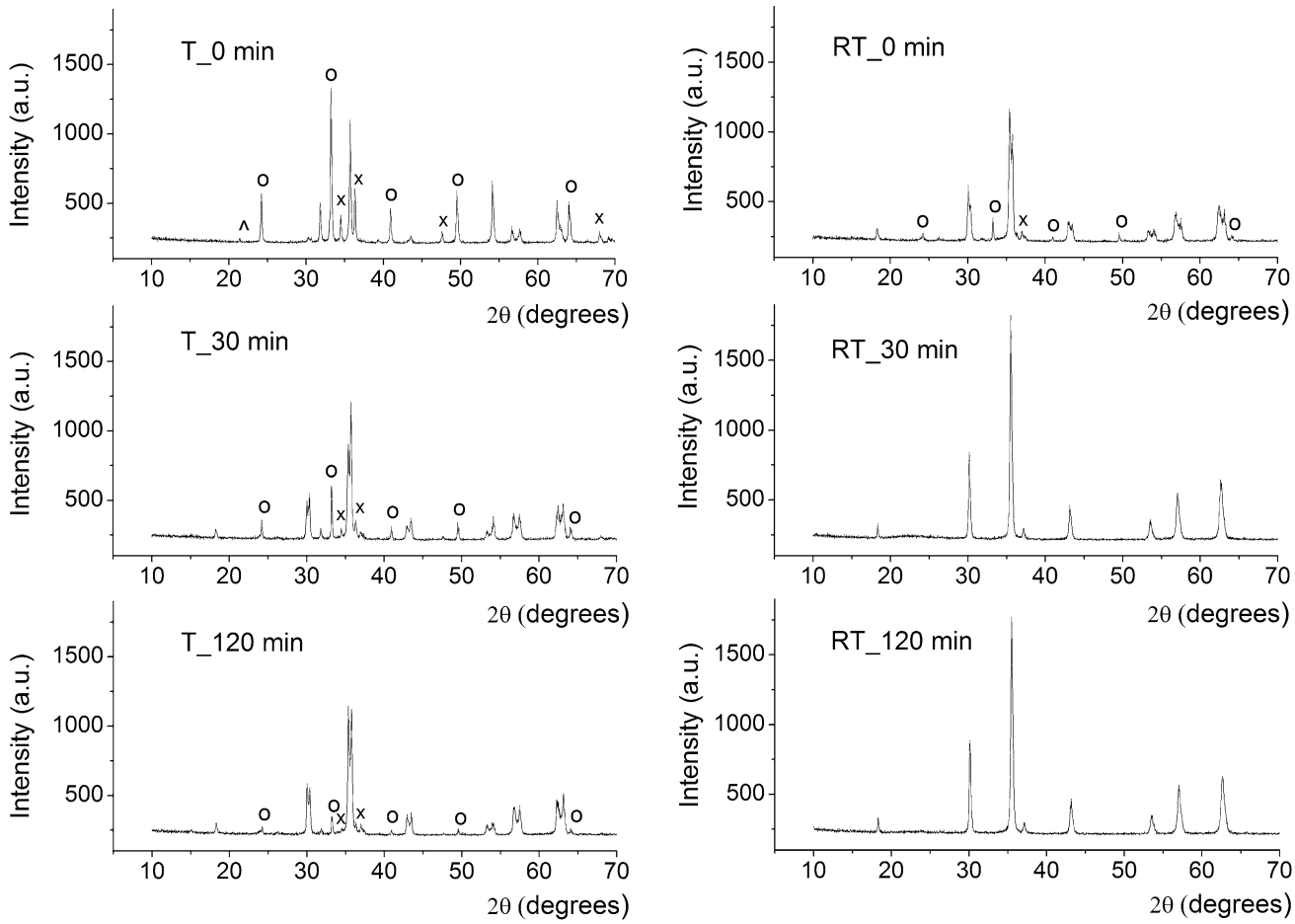

Fig. 6. XRD patterns for $Li_{0.5(1-x)}Zn_xFe_{2.5-0.5x}O_4$ (x = 0.4) synthesized under conditions of T and RT annealing at 750°C and 0 min, 30 min, and 120 min. The markers of Fe_2O_3 (O), Li_2CO_3 (^) and ZnO (x) are indicated.

and, consequently, this can increase the mobility of such ions and accelerate the reaction.

CONCLUSIONS

Lithium-zinc ferrites were studied by XRD and saturation magnetization analysis. The samples were obtained by the conventional thermal synthesis or radiation-thermal synthesis via 2.4 MeV electron beam heating of Li_2CO_3-Fe_2O_3-ZnO powder mixtures.

The obtained results indicate a high efficiency of LiZn ferrite formation using a high-energy electron beam as a heating source for reaction mixtures. Lower temperatures and synthesis time are required to obtain the ferrites with homogenous phase composition by RT compared to standard thermal heating. The radiation effect in the ferrite formation is greatest at the initial isothermal stage of synthesis during mixture heating. Thus, RT synthesis at 750°C and isothermal exposure for 30 min or more form lithium-zinc ferrites with a high degree of final phase composition, which is also characterized by high values of saturation magnetization.

Following,[41] it should be noted that higher temperatures and longer isothermal exposure, including mandatory multiple intermediate grinding and mixing operations, are required to obtain LiZn ferrites with homogeneous phase composition by using conventional thermal synthesis.

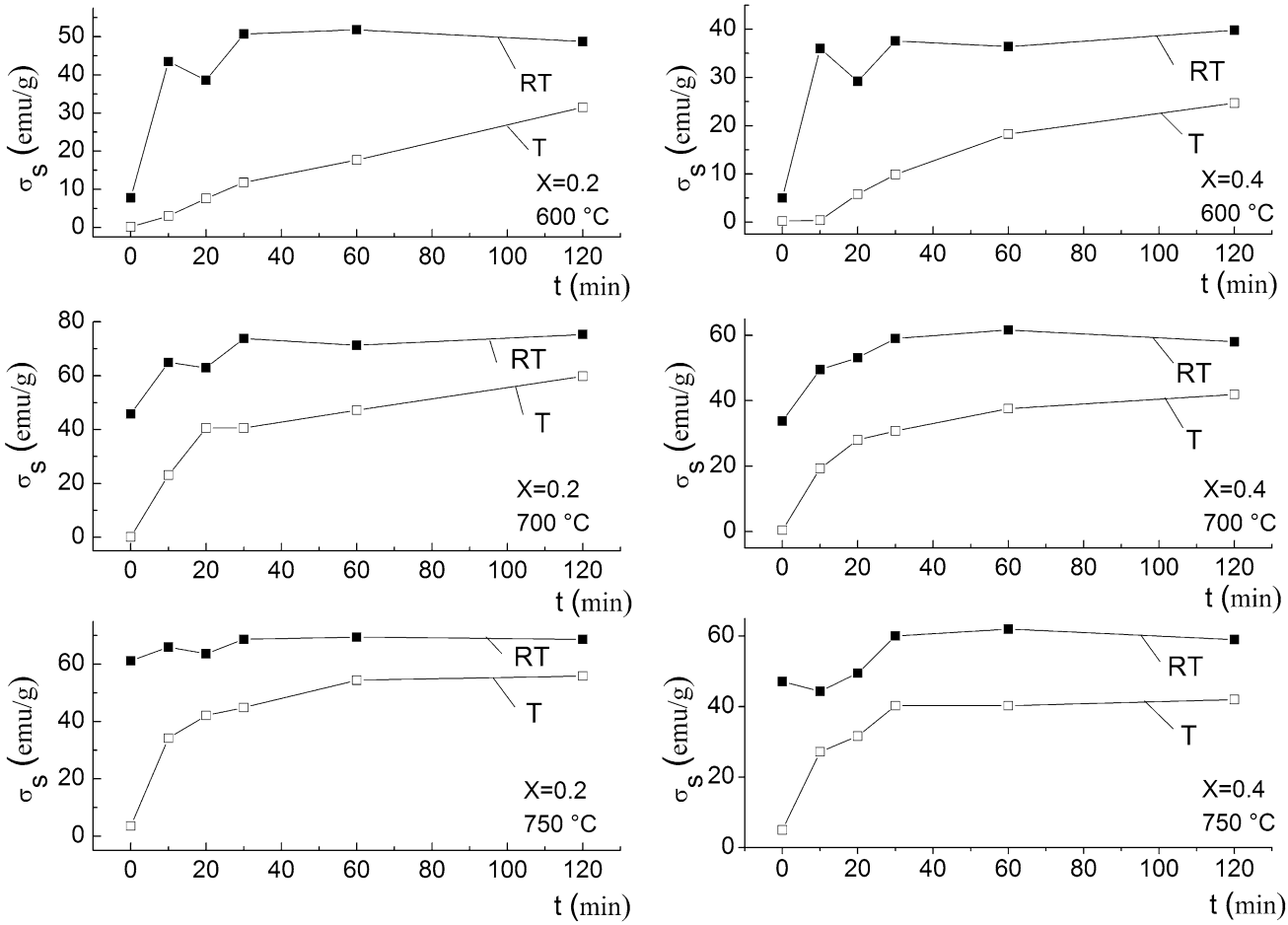

Fig. 7. Saturation magnetization for $Li_{0.5(1-x)}Zn_xFe_{2.5-0.5x}O_4$ (x = 0.2, 0.4) synthesized by T and RT heating versus isothermal exposures of samples during synthesis at 600°C, 700°C, and 750°C annealing temperatures.

ACKNOWLEDGEMENTS

The research is funded by The Ministry of Education and Science of the Russian Federation as part of the "Science" Program, Project 11.980.2017/4.6. The experimental calculations were carried out at Tomsk Polytechnic University within the framework of Tomsk Polytechnic University Competitiveness Enhancement Program Grant. The authors would like to thank Dr. M. Korobeynikov for radiation-thermal measurements.

REFERENCES

1. P.D. Baba, G.M. Argentina, W.E. Courtney, G.F. Dionne, and D.H. Temme, *IEEE Trans. Magn.* 8, 83 (1972).
2. K. Zhou, W. Chen, X. Wu, W. Wu, C. Lin, and J. Wu, *J. Electron. Mater.* 46, 4618 (2017). https://doi.org/10.1007/s11664-017-5466-0.
3. I. Ahmad, S.M. Shah, M.N. Ashiq, F. Nawaz, A. Shah, M. Siddiq, I. Fahim, and S. Khan, *J. Electron. Mater.* 45, 4979 (2016).
4. G.O. White and C.E. Patton, *Magn. Magn. Mater.* 9, 299 (1978).
5. S.H. Gee, Y.K. Hong, M.H. Park, D.W. Erickson, and P.J. Lamb, *J. Appl. Phys.* 91, 7586 (2002).
6. M.S. Ruiz and S.E. Jacobo, *Phys. B* 407, 3274 (2012).
7. M. Kavanlooee, B. Hashemi, H. Maleki-Ghaleh, and J. Kavanlooee, *J. Electron. Mater.* 41, 3082 (2012).
8. S.K. Gurav, S.E. Shirsath, R.H. Kadam, S.M. Patange, K.S. Lohar, and D.R. Mane, *Mater. Res. Bull.* 48, 3530 (2013).
9. A.V. Malyshev, E.N. Lysenko, and V.A. Vlasov, *Ceram. Int.* 41, 13671 (2015).
10. M. Shahjahan, N.A. Ahmed, S.N. Rahman, S. Islam, N. Khatun, and M.S. Hossain, *Int. J. Innov. Techol. Explor. Eng.* 3, 48 (2014).
11. E. De Fazio, P.G. Bercoff, and S.E. Jacobo, *J. Magn. Magn. Mat.* 323, 2813 (2011). https://doi.org/10.1016/j.jmmm.2011.06.022.
12. A.N. Yusoff and M.N. Abdullah, *J. Magn. Magn. Mater.* 269, 271 (2004). https://doi.org/10.1016/S0304-8853(03)00617-6.
13. M. Yasuoka, Y. Nishimura, T. Nagaoka, and K. Watari, *J. Therm. Anal. Calorim.* 83, 407 (2006).
14. A.M. Ibrahim, M.M. Abd El-Latif, and M.M. Mahmoud, *J. Alloy. Compd.* 506, 201 (2010).
15. H.M. Widatallah, X.L. Ren, and I.A. Al-Omari, *J. Mater. Sci.* 41, 6333 (2006).
16. V. Berbenni, A. Marini, P. Matteazzi, R. Ricceri, and N.J. Welham, *J. Eur. Ceram. Soc.* 23, 527 (2003).
17. V.V. Boldyrev, *Russ. Chem. Rev.* 75, 177 (2006).
18. D. Michael, P. Mingos, and D.R. Baghurst, *Chem. Soc. Rev.* 20, 1 (1991).
19. M. Oghbaei and O. Mirzaee, *J. Alloy. Compd.* 494, 175 (2010).

20. N.Z. Lyakhov, V.V. Boldyrev, A.P. Voronin, O.S. Gribkov, I.G. Bochkarev, S.V. Rusakov, and V.L. Auslender, *J. Therm. Anal. Calorim.* 43, 21 (1995).
21. V.V. Boldyrev, A.P. Voronin, O.S. Gribkov, E.V. Tkachenko, G.R. Karagedov, B.I. Yakobson, and V.L. Auslender, *Solid State Ion.* 36, 1 (1989).
22. V.L. Auslender, I.G. Bochkarev, V.V. Boldyrev, N.Z. Lyakhov, and A.P. Voronin, *Solid State Ion.* 101–103, 489 (1997).
23. V.A. Neronov, A.P. Voronin, M.I. Tatarintseva, T.E. Melekhova, and V.L. Auslender, *J. Less Common Metals* 117, 391 (1986).
24. V.G. Kostishin, V.G. Andreev, V.V. Korovushkin, D.N. Chitanov, N.A. Yudanov, A.T. Morchenko, A.S. Komlev, AYu Adamtsov, and A.N. Nikolaev, *Inorgan. Mater.* 50, 1317 (2014).
25. U.V. Ancharova, M.A. Mikhailenko, B.P. Tolochko, N.Z. Lyakhov, M.V. Korobeinikov, A.A. Bryazgin, V.V. Bezuglov, and E.A. Shtarklev *I.O.P. Conf. Ser. Mater. Sci. Eng.* 81, 012122 (2015).
26. V.A. Zhuravlev, E.P. Naiden, R.V. Minin, V.I. Itin, V.I. Suslyaev, and E.Y. Korovin *I.O.P. Conf. Ser. Mater. Sci. Eng.* 81, 012003 (2015). https://doi.org/10.1088/1757-899X/81/1/012003.
27. E.P. Naiden, R.V. Minin, V.I. Itin, and V.A. Zhuravlev, *Russ. Phys. J.* 56, 674 (2013).
28. A.P. Surzhikov, A.M. Pritulov, E.N. Lysenko, A.N. Sokolovskii, V.A. Vlasov, and E.A. Vasendina, *J. Therm. Anal. Calorim.* 110, 733 (2012). https://doi.org/10.1007/s10973-011-1947-1.
29. E.N. Lysenko, A.P. Surzhikov, V.A. Vlasov, E.V. Nikolaev, A.V. Malyshev, A.A. Bryazgin, M.V. Korobeynikov, and M.A. Mikhailenko, *J. Nucl. Instr. Meth. Phys. Res. B.* 392, 1 (2017).
30. A.P. Surzhikov, E.N. Lysenko, V.A. Vlasov, A.V. Malyshev, and E.A. Vasendina, *Mater. Chem. Phys.* 176, 110 (2016).
31. A.V. Malyshev, E.N. Lysenko, V.A. Vlasov, and S.A. Nikolaeva, *Ceram. Int.* 42, 16180 (2016).
32. V.L. Auslender, *J. Nucl. Instr. Meth. Phys. Res. B.* 89, 46 (1994).
33. R.A. Salimov, V.G. Cherepkov, J.I. Golubenko, G.S. Krainov, B.M. Korabelnikov, S.A. Kuznetsov, N.K. Kuksanov, A.B. Malinin, and P.I. Nemytov, *J. Radiat. Phys. Chem.* 57, 661 (2000).
34. V.V. Bezuglov, A.A. Bryazgin, A.Y. Vlasov, E.N. Kokin, and E.A. Shtarklev, *Phys. Part. Nucl. Lett.* 13, 784 (2016).
35. E.W. Gorter, *J. Philips Res. Rep.* 9, 295 (1954).
36. C.E. Patton, C.A. Edmondson, and Y.H. Liu, *J. Appl. Phys.* 53, 2431 (1982).
37. W.D. Wilber, P. Kabos, and C.E. Patton, *IEEE Trans. Magn.* 19, 1862 (1983). https://doi.org/10.1109/TMAG.1983.1062727.
38. S. Misra, S. Ram, and R.S. Shinde, *AIP Conf. Proc.* 1447, 413 (2012). https://doi.org/10.1063/1.4710055.
39. J. Sláma, M. Šoka, A. Grusková, R. Dosoudil, V. Jančárik, and J. Degmová, *J. Magn. Magn. Mater.* 326, 251 (2013). https://doi.org/10.1016/j.jmmm.2012.07.016.
40. Y.M. Annenkov, *Russ. Phys. J.* 39, 1146 (1996).
41. A.P. Surzhikov, A.M. Pritulov, E.N. Lysenko, V.A. Vlasov, E.A. Vasendina, and A.V. Malyshev, *J. Therm. Anal. Calorim.* 112, 739 (2013).